Bonding Study in All-Metal Clusters Containing Al₄ Units

Marcos Mandado,*,† Alisa Krishtal,‡ Christian Van Alsenoy,‡ Patrick Bultinck,§ and J. M. Hermida-Ramón†

Department of Physical Chemistry, University of Vigo, As Lagoas (Marcosende) sn, 36310 Vigo, Galicia, Spain, Department of Chemistry, University of Antwerp, Universiteitsplein 1, B-2610 Wilrijk, Belgium, and Department of Inorganic and Physical Chemistry, Ghent University, Krijgslaan 281 (S-3), B-9000 Gent, Belgium

The nature of the bonding of a series of gas-phase all-metal clusters containing the Al₄ unit attached to an alkaline, alkaline earth, or transition metal is investigated at the DFT level using Mulliken, quantum theory of atoms in molecules (QTAIM), and Hirshfeld iterative (Hirshfeld-I) atomic partitionings. The characterization of ionic, covalent, and metallic bonds is done by means of charge polarization and multicenter electron delocalization. This Article uses for the first time Hirshfeld-I multicenter indices as well as Hirshfeld-I based atomic energy calculations. The QTAIM charges are in line with the electronegativity scale, whereas Hirshfeld-I calculations display deviations for transition metal clusters. The Mulliken charges fail to represent the charge polarization in alkaline metal clusters. The large ionic character of Li−Al and Na−Al bonds results in weak covalent bonds. On the contrary, scarcely ionic bonds (Be−Al, Cu−Al and Zn−Al) display stronger covalent bonds. These findings are in line with the topology of the electron density. The metallic character of these clusters is reflected in large 3-, 4- and 5-center electron delocalization, which is found for all the molecular fragments using the three atomic definitions. The previously reported magnetic inactivity (based on means of magnetic ring currents) of the π system in the Al₄²⁻ cluster contrasts with its large π electron delocalization. However, it is shown that the different results not necessary contradict each other.

1. Introduction

The discovery of aromatic/antiaromatic behavior of gas-phase metal clusters has given rise to an ever growing number of studies of their properties. Among the most important papers, especially the ones by Kuznetsov et al.[1,2] and the review by Boldyrev and Wang[3] have contributed to the interest in these systems.

Kuznetsov et al. first made a series of bimetallic clusters, Al₄Li⁻, Al₄Na⁻ and Al₄Cu⁻, in the gas phase and obtained their photoelectron spectra.[1] They also performed a theoretical study pointing out that the most stable isomers of these bimetallic clusters all contain a square-planar Al₄²⁻ dianion, which was shown to be simultaneously π and σ aromatic. Consequently, they extended the concept of aromaticity to all-metal clusters. Since then, the aromaticity of the Al₄²⁻ dianion has been studied using different criteria; maps of ring currents,[4−7] aromatic ring current shieldings (ARCS),[8,9] nuclear independent chemical shifts (NICS),[10] induced magnetic field analysis,[11] valence bond calculations (VB),[12] bifurcation analysis of the electron localization function (ELF),[13] resonance energy estimations (RE)[14,15] and conceptual DFT descriptors.[16] Also, the aromaticity/antiaromaticity of a large number of new gaseous all-metal or metalloid clusters has been investigated: X₄²⁻ (X = B, Al, Ga, In, Tl),[8,9,14,15,17,18] Si₂X₂ (X = B, Al, Ga),[8,9] XAl₃⁻ (X = C, Si, Ge, Sn, Pb),[19] XGa₃⁻ (X = Si, Ge),[20] NaGa₄⁻ and NaIn₄⁻,[18,21] X₃⁻ and NaX₃ (X = Al, Ga),[22] Au₅Zn⁺,[23−25] CuₙHₙ (n =

3−6),[26] sandwich structures of [Al₄TiAl₄]²⁻ and Na[Al₄TiAl₄]⁻,[27] Al₂(CO)₂,[28] X₄²⁻ and NaX₄⁻ (X = N, P, As, Sb, Bi),[29] X₅⁻ (X = N, P, As, Sb, Bi),[28−33] and Al₄Na₄ and Al₄Na₃⁻.[34] In the works by Tsipis[35] and Nigam et al.,[36] the aromaticity of a large variety of charged and neutral tetramer cluster is investigated and deserves mention. Obviously, the vague definition of aromaticity has already given rise to sometimes conflicting conclusions for all metal clusters. It is therefore important to stress that in the following, aromaticity should be considered the presence of a delocalized electronic system, except if explicitly mentioned otherwise.

A previous study using electron localization function, ELF, indicated the presence of multicenter bonding in the Al₄X₄ (X = Be, Mg, B, Si) clusters.[37] In the same work, Shetty et al. detected large ionic character in small Sn-doped Li clusters. Unfortunately, the ELF method does not provide quantitative information about the extension of the multicenter bonding to different molecular fragments. Here we employ a quantitative tool, the multicenter delocalization indices, using different atomic partitioning schemes, to study the bonding in several all-metal clusters containing the Al₄ fragment.

Electron delocalization indices,[38] also referred to as covalent bond orders,[39,40] are nowadays accepted as a good estimator of the covalent character of traditional 2-center bonds. Also, when its definition is extended to more than two atoms, they are called multicenter delocalization indices or multicenter bond orders. The multicenter delocalization indices were formerly shown to be a powerful tool for characterizing three-center bonds[41−45] and at a later stage proposed as a measure of the multicenter π electron delocalization in cyclic aromatic hydrocarbons.[46−48] More recently, Bultinck et al.[49−55] and Mandado et al.[56−60] have

* Corresponding author. Fax: (+34) 986812321. E-mail address: mandado@uvigo.es.
† University of Vigo.
‡ University of Antwerp.
§ Ghent University.

11886 *J. Phys. Chem. A, Vol. 111, No. 46, 2007*

Mandado et al.

extended the application of multicenter delocalization indices into the study of local and total aromaticity of polycyclic aromatic hydrocarbons,[49−51,53,54,56,57,59] aromaticity of heterocycles,[58] homoaromaticity,[52,55] and concerted reaction mechanisms.[60]

In this work the multicenter delocalization analysis is shown to provide valuable quantitative information about the covalent metal−metal bonding and the multicenter bonding in different molecular fragments. This is the first time that multicenter delocalization indices are computed using the Hirshfeld atomic partitioning. Also, a brief discussion of the σ and π local aromaticity of the Al_4 unit in terms of multicenter electron delocalization is included and compared to previously reported results.

The atomic charge polarization, related to the ionic character of the bond, is also investigated using the Mulliken,[61] quantum theory of atoms in molecules (QTAIM),[62] and Hirshfeld[63] iterative (Hirshfeld-I) atomic partitioning schemes. The applicability of different schemes to describe the charge distribution in these metal clusters is discussed. The partitioning of the total molecular energy into molecular fragment energies is performed using QTAIM and Hirshfeld-I. For the latter a detailed study of intra-atomic and interatomic energy terms is carried out, showing large differences between transition metals and alkaline or alkaline earth metals. It must be remarked that this is first time that Hirshfeld atomic energies are computed at the DFT level of theory.

The paper is organized as follows: In the second section multicenter indices are briefly reviewed. Also, the calculation of DFT atomic energies using Hirshfeld atomic partitioning is introduced. The computational details are presented in section III. The "Results and Discussion" section (section IV) is split into four different parts: the first is devoted to the study of the electron charge polarization (the ionic character of the bonds), the second deals with the analysis of the electron delocalization (covalent and metallic character of the bonds), in the third the local aromaticity of the Al_4 units is studied in detail through the analysis of the multicenter delocalization indices, and some results obtained from the atomic energy decomposition are discussed in the fourth. Finally, the conclusions are formulated.

II. Theoretical Background

Multicenter Delocalization Indices. Given an atomic partitioning of the molecular electron density, the multicenter delocalization indices represent the extent to which the electrons are delocalized among a set of n atoms. Using the Mulliken partitioning scheme,[61] the n-center delocalization index (n-DI) adopts the expression given by[64,65]

$$\Delta_n = 2n \sum_P [\sum_{i \in A} \sum_{j \in B} \sum_{k \in C} \cdots \sum_{m \in M} (P^\alpha S)_{ij}(P^\alpha S)_{jk}\cdots(P^\alpha S)_{mi} + \sum_{i \in A} \sum_{j \in B} \sum_{k \in C} \cdots \sum_{m \in M} (P^\beta S)_{ij}(P^\beta S)_{jk}\cdots(P^\beta S)_{mi}] \quad (1)$$

in which $\mathbf{P}^\alpha$ and $\mathbf{P}^\beta$ are the so-called α and β density matrices and $\mathbf{S}$ is the overlap matrix in terms of basis functions, $i, j, ...$. The first summation in (1) runs over all the nonequivalent permutations P of the n atoms. The remaining summations run over the basis functions centered on the atoms A, B, etc.

When the quantum theory of atoms in molecules (QTAIM)[62] is employed, the n-DI is readily written in terms of molecular spin orbitals

$$\Delta_n = 2n \sum_P [\sum_i^{n_{occ}^\alpha} \sum_j^{n_{occ}^\alpha} \sum_k^{n_{occ}^\alpha} \cdots \sum_m^{n_{occ}^\alpha} \int_A \phi_i(\vec{r}) \phi_j(\vec{r}) \, d\vec{r} \int_B \phi_j(\vec{r})$$

$$\phi_k(\vec{r}) \, d\vec{r} \cdots \int_M \phi_m(\vec{r}) \phi_i(\vec{r}) \, d\vec{r} + \sum_i^{n_{occ}^\beta} \sum_j^{n_{occ}^\beta} \sum_k^{n_{occ}^\beta} \cdots \sum_m^{n_{occ}^\beta} \int_A$$

$$\phi_i(\vec{r}) \phi_j(\vec{r}) \, d\vec{r} \int_B \phi_j(\vec{r}) \phi_k(\vec{r}) \, d\vec{r} \cdots \int_M \phi_m(\vec{r}) \phi_i(\vec{r}) \, d\vec{r}] \quad (2)$$

where the overlap integrals between two molecular spin orbitals, $\phi_i(\vec{r})$ and $\phi_j(\vec{r})$, are performed within the QTAIM atomic basins of the atoms A, B, etc. n_{occ}^α and n_{occ}^β represent the number of occupied α and β spin orbitals, respectively. Expression 2 is the extension of the delocalization indices idea of Bader[38] for the multicenter case.

On the other hand, when the Hirshfeld atomic partitioning scheme[60] is employed, eq 2 turns into

$$\Delta_n = 2n \sum_P [\sum_i^{n_{occ}^\alpha} \sum_j^{n_{occ}^\alpha} \sum_k^{n_{occ}^\alpha} \cdots \sum_m^{n_{occ}^\alpha} \int w_A(\vec{r}) \phi_i(\vec{r}) \phi_j(\vec{r}) \, d\vec{r} \int$$

$$w_B(\vec{r}) \phi_j(\vec{r}) \phi_k(\vec{r}) \, d\vec{r} \cdots \int w_M(\vec{r}) \phi_m(\vec{r}) \phi_i(\vec{r}) \, d\vec{r} +$$

$$\sum_i^{n_{occ}^\beta} \sum_j^{n_{occ}^\beta} \sum_k^{n_{occ}^\beta} \cdots \sum_m^{n_{occ}^\beta} \int w_A(\vec{r}) \phi_i(\vec{r}) \phi_j(\vec{r}) \, d\vec{r} \int w_B(\vec{r}) \phi_j(\vec{r})$$

$$\phi_k(\vec{r}) \, d\vec{r} \cdots \int w_M(\vec{r}) \phi_m(\vec{r}) \phi_i(\vec{r}) \, d\vec{r}] \quad (3)$$

where now the integrals run over the whole space, and the atomic domain of atom A is defined through the atomic weight factor w_A.

All the expressions above are based on monodeterminantal wavefunctions. As such, they are restricted to Hartree−Fock calculations and, in principle, also to Density Functional Theory in the Kohn−Sham approach. In the latter case, however, the wave function strictly refers to independent electrons and as such application of the multicenter index expressions above is not strictly justified. Nevertheless, DFT based delocalization indices have been shown on numerous occasions to give chemically significant results.[66]

Hirshfeld-DFT Atomic Energy Partitioning. The Hirshfeld atomic energy is obtained by partitioning the different one- and two-electron contributions to the total energy. For one-electron contributions, such as the kinetic energy, this is accomplished by introducing the atomic weight factor w_A into the appropriate integral. The contribution of atom A to the total kinetic energy is thus given by

$$E_{kin}^A = \int d\vec{r} \, w_A(\vec{r}) \sum_i \left[-\frac{1}{2} (\vec{\nabla} \phi_i(\vec{r}))^2 \right] \quad (4)$$

The partitioning of DFT-related one-electron integrals, describing exchange and correlation contributions to the total energy, is performed in a similar fashion:

$$E_{xc}^A = \int d\vec{r} \, w_A(\vec{r}) \, \epsilon_{xc}(\rho(\vec{r})) \, \rho(\vec{r}) \quad (5)$$

where ϵ_{xc} represents the actual functional used.

The partitioning of two-electron contributions is slightly more complicated, as they involve integration over the coordinates of two electrons. In this case, a separate weight function must be employed for each electron. For example, the contribution of atoms A and B to the coulomb interaction energy is given by

All-Metal Clusters Containing Al$_4$

J. Phys. Chem. A, Vol. 111, No. 46, 2007 **11887**

$$E_{\text{Coulomb}}^{\text{AB}} = \sum_{i<j} \int d\vec{r}_1\, w_A(\vec{r}_1) \int d\vec{r}_2\, w_B(\vec{r}_2)$$

$$\phi_i^2(\vec{r}_1) \frac{1}{|\vec{r}_1 - \vec{r}_2|} \phi_j^2(\vec{r}_2) \quad (6)$$

The exchange contributions are partitioned in a similar manner. Further details of this partitioning scheme can be found in ref 67. For hybrid DFT functionals such as B3LYP, the one-electron terms are partitioned according to eq 5 and the Coulomb and exchange terms are partitioned according to eq 6.

The partitioning of the HF and DFT molecular energy into atomic contributions leads initially to a sum of one-center and two-center energy terms,[68−74] depending on whether one atom or two atoms are involved in the calculation of the core-attraction, Coulomb, exchange and nuclear repulsion terms. Using symmetrized expressions for the core-attraction energy between two different atoms,[68] the initial partitioning of the total energy into one-center and two-center terms can be expressed by a sum of atomic terms.

III. Computational Details

The DFT level of calculation, with the B3LYP hybrid functional and the 6-311+G(d) basis set, was employed for the geometry optimizations and wave function calculations. The geometries and frequencies obtained with this method were shown to be in good agreement with those obtained with the MP2, CASSCF, or CCSD(T) methods.[1,14,21] Also, theoretical vertical detachment energies obtained with the B3LYP/6-311+G(d) method were shown to be in good agreement with experimental data.[1] All DFT calculations were performed using the Gaussian 03 program.[75] The calculations of the QTAIM atomic charges and energies were performed using the AIMPAC package of programs.[76] The QTAIM atomic energies were computed from the atomic kinetic energies using the molecular virial ratio.[62] The calculations of the Hirshfeld atomic charges and energies were carried out with the BRABO package of programs.[77,78] The calculations of multicenter indices were carried out using a self-written FORTRAN program. AIMPAC and BRABO were employed to obtain the QTAIM and Hirshfeld overlap integrals within the atomic domains, respectively. The topological analysis of the electron density and characterization of bond, ring and cage critical points (BCPs, RCPs, and CCPs, respectively) were performed using the AIM2000 program.[79]

Recently, two of us introduced a new iterative Hirshfeld atomic partitioning scheme,[80] referred to as Hirshfeld-I, based on the maximal conservation of the entropic information of the isolated atoms in the atoms-in-molecules. This new procedure avoids some problems concerning the promolecular density that affect charged molecules [see refs 80 and 81 for details]. Because most of the metal clusters studied here are negatively charged, this new procedure has been employed to calculate the Hirshfeld n-DIs, charges, and atomic energies.

IV. Results and Discussion

Electron Charge Polarization. The optimized geometries of the most stable conformers of the studied metal clusters are shown in Figure 1. The molecular symmetry and spin multiplicity (singlet for all molecules) are also included in the figure. As one can see, the energy minima of Al$_4$Li$^-$, Al$_4$Na$^-$, Al$_4$Mg, and Al$_4$Cu$^-$ correspond to the C_{4v} symmetry group, displaying four equivalent M−Al and Al−Al distances. These structures were previously obtained using the same level as well as other levels of theory (see ref 3 and references therein). On the
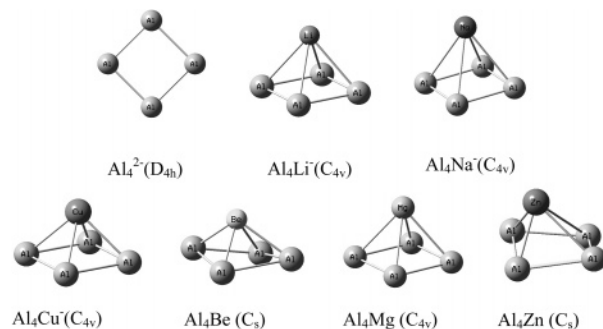
Figure 1. Molecular geometry and symmetry of all-metal clusters studied.

TABLE 1: Charges of the Al$_4$ and M Fragments in All-Metal Clusters Studied (Figure 1)^a

	Al$_4$Li$^-$	Al$_4$Na$^-$	Al$_4$Cu$^-$	Al$_4$Be	Al$_4$Mg	Al$_4$Zn
Q(Al$_4$)	−1.748	−1.512	−0.335	0.398	−0.700	0.158
	−1.533	−1.498	−1.119	0.038	−0.523	−0.225
	−0.729	−0.776	−0.552	0.333	0.125	0.226
Q(M)	0.748	0.512	−0.665	−0.398	0.700	−0.158
	0.533	0.498	0.119	−0.038	0.523	0.225
	−0.271	−0.224	−0.448	−0.333	−0.125	−0.226

^{a} The first, second, and third numbers are respectively the QTAIM, Hirshfeld-I, and Mulliken values.

contrary, the energy minima of Al$_4$Be and Al$_4$Zn correspond to the C_s symmetry group. These clusters display two equivalent M−Al distances, the other two M−Al distances are one significantly shorter and the other one longer than the rest. These clusters also display pairs of equivalent Al−Al distances.

Table 1 collects the QTAIM, Hirshfeld-I, and Mulliken charges of the Al$_4$ and M fragments. The QTAIM charges are more in line with the electronegativity criterion. Thus, the charge is always polarized from the least to the most electronegative atoms according to QTAIM. The Hirshfeld-I charges only disagree with the QTAIM ones for the transition metal clusters, especially for the Al$_4$Cu$^-$. According to Hirshfeld-I the negative charge is located at the Al$_4$ unit, whereas the Cu atom displays a small positive charge, contradicting the electronegativity criterion. On the contrary, Mulliken charges coincide with the QTAIM ones for the transition metal clusters and Al$_4$Be. According to Mulliken the charge polarization is unnoticeable in alkaline metal clusters, the total negative charge being shared by all the atoms according to the Mulliken charges. This also contradicts the results obtained for small Li$_n$Sn clusters using ELF.[37] This shows that the Mulliken approach, in the present case, fails. This may be due to the use of diffuse functions for which it is known that the Mulliken approach does not perform well.[82] On the other hand, the polarity of the present molecules may also cause problems with this scheme.[83]

According to the QTAIM and Hirshfeld-I charges the Al$_4$Li$^-$ and Al$_4$Na$^-$ clusters and to a lesser extent the Al$_4$Mg cluster display a large charge polarization from the metal M to the Al$_4$ fragment. This large charge polarization indicates an important ionic character of the M−Al bonds.

As a common point of the three atomic partitionings, the most electron deficient Al$_4$ fragments correspond to the C_s clusters, Al$_4$Be and Al$_4$Zn. The QTAIM and Mulliken charges indicate that the Al$_4$ fragments are positively charged in these clusters, whereas according to Hirshfeld-I they display small positive and negative charges in Al$_4$Be and Al$_4$Zn, respectively. It must be noticed that an electron transfer from Be to Al atoms was previously proposed in the Al$_4$Be$_4$ system using ELF.[37] How-

TABLE 2: Multicenter Bond Indices for Different Molecular Fragments of the C_{4v} All-Metal Clusters and the Al_4^{2-} Cluster[a]

	Al——M	M / Al——Al	M / Al-Al-Al	M / Al-Al-Al-Al	Al——Al	Al-Al / Al-Al	Al——Al / Al——Al
Al_4^{2-}					1.0651(0.8012)	0.3875	0.3417
					1.3608(0.8980)	0.4901	0.3726
					1.1239(0.6482)	0.3612	0.3350
Al_4Li^-	0.1207	0.0721(0.0697)	0.0594	0.0684	1.0211(0.7585)	0.3423	0.2866
	0.2549	0.1335(0.1104)	0.0886	0.0914	1.2392(0.8055)	0.3960	0.2699
	0.4257	0.1278(0.1740)	0.0820	0.1218	0.6355(0.6185)	0.1507	0.2051
Al_4Na^-	0.2071	0.1123(0.1075)	0.0831	0.0857	0.9670(0.7060)	0.2958	0.2339
	0.2954	0.1411(0.1224)	0.0942	0.0933	1.2157(0.7787)	0.3733	0.2464
	0.3600	0.0867(0.1462)	0.0599	0.1108	0.6340(0.6200)	0.1640	0.2285
Al_4Cu^-	0.6266	0.2078(0.1114)	0.0835	0.0597	0.7375(0.5375)	0.1736	0.1277
	0.7789	0.2442(0.1508)	0.1085	0.0834	1.0255(0.6422)	0.2650	0.1576
	0.4481	0.1658(0.0558)	0.0784	0.0249	0.7029(0.5071)	0.1361	0.1307
Al_4Mg	0.3853	0.1535(0.1313)	0.0786	0.0655	0.8336(0.5975)	0.2125	0.1533
	0.5339	0.2244(0.1659)	0.1043	0.0800	1.0005(0.6350)	0.2501	0.1447
	0.4169	0.0969(0.1170)	0.0640	0.0796	0.5373(0.5341)	0.1208	0.1665

[a] The first, second, and third numbers are respectively the QTAIM, Hirshfeld-I, and Mulliken values. The numbers in Parentheses correspond to molecular fragments that define a vertical symmetry plane.

TABLE 3: Multicenter Bond Indices, Δ_n, for Different Molecular Fragments in Al_4Be and Al_4Zn[a]

	$\Delta_2^{12} = \Delta_2^{23}$	Δ_2^{13}	$\Delta_2^{14} = \Delta_2^{34}$	Δ_2^{24}
	0.7258	0.4937	0.5933	0.4456
	0.9456	0.6133	0.8495	0.5050
	0.5781	0.4762	0.5109	0.4223
$\Delta_2^{15} = \Delta_2^{35}$	Δ_2^{25}	Δ_2^{45}	Δ_3^{123}	$\Delta_3^{124} = \Delta_3^{234}$
0.6933	0.3935	1.0862	0.1066	0.1178
0.7398	0.3994	1.0836	0.1863	0.1864
0.5354	0.3507	0.9232	0.0073	0.1269
Δ_3^{134}	$\Delta_3^{125} = \Delta_3^{235}$	$\Delta_3^{145} = \Delta_3^{345}$	Δ_3^{135}	Δ_3^{245}
0.1518	0.1545	0.3761	0.1641	0.2194
0.2421	0.1896	0.4312	0.2167	0.2218
0.0945	0.1176	0.3078	0.0818	0.1953
Δ_4^{1234}	Δ_4^{1235}	$\Delta_4^{1245} = \Delta_4^{2345}$	Δ_4^{1345}	Δ_5^{12345}
0.0712	0.0713	0.1125	0.1364	0.0749
0.1005	0.0915	0.1299	0.1752	0.0944
0.1066	0.0628	0.1110	0.1117	0.0822
	$\Delta_2^{12} = \Delta_2^{23}$	Δ_2^{13}	$\Delta_2^{14} = \Delta_2^{34}$	Δ_2^{24}
	0.7490	0.5121	0.6897	0.4697
	0.9444	0.5902	0.9127	0.5297
	0.6016	0.4934	0.5830	0.4532
$\Delta_2^{15} = \Delta_2^{35}$	Δ_2^{25}	Δ_2^{45}	Δ_3^{123}	$\Delta_3^{124} = \Delta_3^{234}$
0.4809	0.2629	0.8334	0.1463	0.1550
0.6033	0.3005	1.0262	0.2020	0.2072
0.2976	0.2165	0.6537	0.0483	0.1681
Δ_3^{134}	$\Delta_3^{125} = \Delta_3^{235}$	$\Delta_3^{145} = \Delta_3^{345}$	Δ_3^{135}	Δ_3^{245}
0.1691	0.0972	0.2522	0.1098	0.1610
0.2348	0.1205	0.3101	0.1443	0.1663
0.0881	0.0748	0.1896	0.0497	0.1497
Δ_4^{1234}	Δ_4^{1235}	$\Delta_4^{1245} = \Delta_4^{2345}$	Δ_4^{1345}	Δ_5^{12345}
0.1092	0.0543	0.1125	0.0822	0.0625
0.1193	0.0617	0.0911	0.1198	0.0675
0.1271	0.0598	0.0895	0.0868	0.0594

[a] The first, second, and third numbers are respectively the QTAIM, Hirshfeld-I, and Mulliken values.

ever, that contradicts the atomic charges obtained with Mulliken, QTAIM and Hirshfeld-I, which suggest the contrary.

Multicenter Bonding Analysis and Electron Density Topology. Tables 2 and 3 collect the *n*-DIs ($n = 2-5$) for all the non-symmetrical molecular fragments contained in the metal clusters. Table 2 collects the values for the C_{4v} clusters, whereas Table 3 collects the values for the C_s clusters.

Let us discuss first the results obtained for the series of C_{4v} clusters. The QTAIM and Hirshfeld-I 2-DIs show large differ-

ences with the Mulliken ones. The values for the Cu−Al bonds are quite close to that of a single bond (0.6266 and 0.7789 using QTAIM and Hirshfeld-I, respectively) and are also close to that of the Al−Al bonds in the same cluster (0.7375 and 1.0255 using QTAIM and Hirshfeld-I, respectively). The values for Li−Al and Na−Al bonds are significantly smaller, indicating a much weaker covalent bond. Also, the Al−Al bonds in Al_4Li^- and Al_4Na^- are stronger than the rest, approaching the values in the Al_4^{2-}. The values for Mg−Al are between those of Na−Al and Cu−Al using QTAIM and Hirshfeld-I. It is noticeable that no significant differences are found along the series using Mulliken scheme, displaying values between 0.3600 and 0.4481 for Na−Al and Cu−Al, respectively. On the other hand, the Mulliken Al−Al 2-DIs are smaller than the corresponding QTAIM and Hirshfeld-I values. These differences found between Mulliken and QTAIM/Hirshfeld-I 2-DIs are a consequence of the small Mulliken electron charge polarization in alkaline metal clusters.

The QTAIM, Hirshfeld-I, and Mulliken results reflect a significant three-center bonding in the MAl_2 fragments for all clusters, being especially large in the Al_4Cu^-. Remarkably, the QTAIM 3-DI of the $CuAl_2$ fragments is even larger than those of the Al_3 fragments. Once again, the smallest values are displayed by the $LiAl_2$ and $NaAl_2$ fragments according to QTAIM and Hirshfeld-I. The QTAIM value for $MgAl_2$ is between that of $CuAl_2$ and $NaAl_2$, whereas the Hirshfeld-I value for this fragment approaches to that of $CuAl_2$. Mulliken values display again deviations for the alkaline metal clusters; although the larger 3-DI corresponds to the $CuAl_2$, it is followed by that of $LiAl_2$.

The 4-DIs and 5-DIs for MAl_3 and MAl_4 fragments, respectively, have the same order of magnitude. To estimate the relative weight of the electron delocalization for multiple centers in metal clusters, one can compare for instance the QTAIM 4-DI and 5-DI values from Tables 2 and 3 with those of highly delocalized π systems like $C_4H_4^{2+}$ and $C_5H_5^-$, which are 0.180 and 0.042, respectively. The 4-DIs of the MAl_3 fragments display values that are smaller than that of the $C_4H_4^{2+}$ yet considerably large. On the other hand, the values of 5-DIs for the MAl_4 fragments are larger than that of the $C_5H_5^-$, which denotes the large extension of the electron delocalization in these metallic compounds. On the other hand, although the 4-DI of the Al_4 fragment is always larger than those of the MAl_3 fragments, its difference drastically reduces in Al_4Cu^-. This is
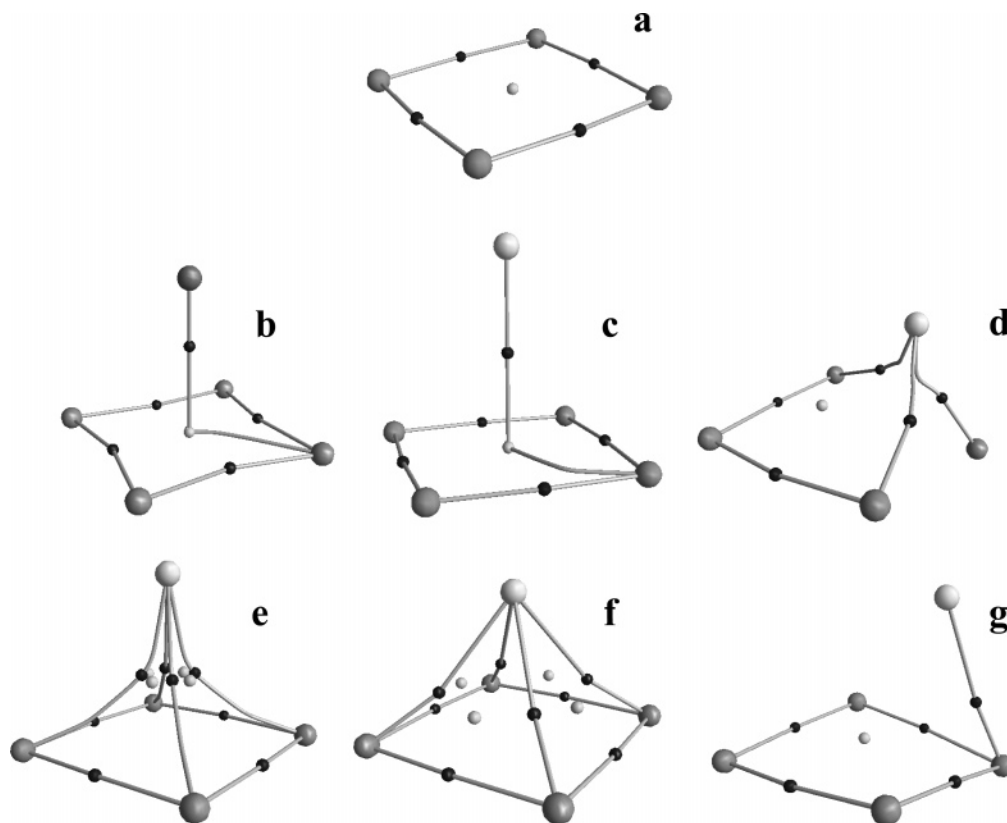
Figure 2. Plot of critical points found in the all-metal clusters studied: (a) Al42-; (b) Al4Li-; (c) Al4Na-; (d) Al4Be; (e) Al4Mg; (f) Al4Cu-; (g) Al4Zn. Small black dots represent bond critical points, BCPs, and small white dots represent ring critical points, RCPs. No cage critical points, CCPs, were found.

due to the decrease in the electron delocalization of pure aluminum fragments when the electron delocalization of M containing fragments increases. This fact was first noticed in polycyclic aromatic hydrocarbons,[56,57] where the extension of the π electron delocalization to neighboring rings results in a decrease of the local ring π electron delocalization.

The *n*-DIs for Al$_4$Be and Al$_4$Zn are collected in Table 3. These compounds display a large geometry distortion, which can be understood in terms of electron delocalization. The Be and Zn atoms approach one of the Al atoms, to which they are strongly covalently bonded. As result, the corresponding 2-DI for that bond is the largest one according to the three atomic partitionings, even larger than those for Al−Al bonds, which explains the proximity of these metals to one of the Al atoms. Also, the 3-DIs and 4-DIs of fragments containing these two atoms (numbered as atoms 2 and 3 in the table) are the largest ones, reflecting also the large metallic character of these clusters. All of this is in line with a preference for the M−Al bonding instead of the Al−Al when M = Be and Zn.

The large multicenter electron delocalization, which is present in all molecular fragments containing three, four, and five centers, agrees with the large electron sharing associated to the metallic bonding. This is another proof of the ability of multicenter delocalization analysis to detect multicenter bonding, even in the particular case of metals.

To get an image of the bonding we have determined the topology of the electron density and plotted the BCPs, RCPs, and CCPs. Figure 2 clearly shows the atypical topology displayed by these metal clusters. It must be noticed that no CCPs have been found in these systems, and that the Poincaré−Hof relation is satisfied so that the set of critical points found is complete. The information obtained from Figure 2 agrees with the conclusions derived from the atomic charge and multicenter

electron delocalization analysis. Thus, the topological features of C_{4v} clusters are very different between clusters with large ionic M−Al bonds (M = Li, Na) and large covalent M−Al bonds (M = Cu). The former do not display BCPs linked the aluminum atoms and the metal, but they show a BCP placed on the symmetry axis connecting the metal and one of the Al atoms and passing through the RCP of the Al$_4$ ring. On the contrary, the Al$_4$Cu$^-$ cluster shows four BCPs connecting the metal with all the aluminum atoms and the corresponding RCPs of the Al$_2$M rings. Moreover, in this cluster the RCP corresponding to the Al$_4$ ring disappears. An intermediate behavior is displayed by the Al$_4$Mg cluster. In this cluster the BCPs connecting the metal with the aluminum atoms and the corresponding RCPs still remain, although they are close to collapsing. For this cluster, the RCP corresponding to the Al$_4$ ring also disappears.

Much more atypical is the topology of the C_s clusters. The Al$_4$Be shows BCPs connecting the metal and all the aluminum atoms, whereas the Al$_4$Zn only displays the BCP corresponding to the bond between the metal and the nearest aluminum. This is explained by the smaller 2-DIs displayed in the Al$_4$Zn cluster with respect to the same atom pairs in Al$_4$Be. On the other hand, all the BCPs connecting two aluminum atoms remain in the Al$_4$Zn cluster, whereas two of them (those with smallest 2-DIs) disappear in the Al$_4$Be. Once more, this difference can be explained by the values of 2-DIs, where the smallest values of the Al−Al pairs correspond to the Al$_4$Be cluster.

Local Aromaticity of the Al$_4$ Unit. The Al$_4$ molecular fragment merits special attention because its σ and π aromatic character has been already studied in the literature (see introduction). In this subsection we try to give extra information about the σ and π local aromaticity of the Al$_4$ unit in metal complexes using multicenter electron delocalization indices. Havenith et

Al_4^{2-} Al_4Li^- Al_4Na^- Al_4Cu^- Al_4Mg
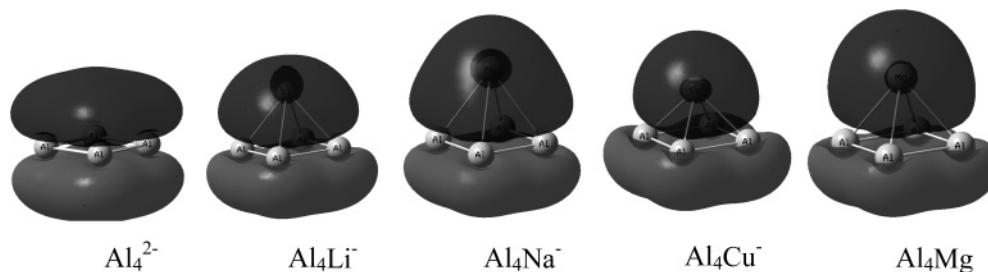
Figure 3. Plots of the Kohn−Sham π molecular orbitals corresponding to the valence shell of the all-metal clusters studied. The nodal plane of the π system corresponds to the Al_4 plane.
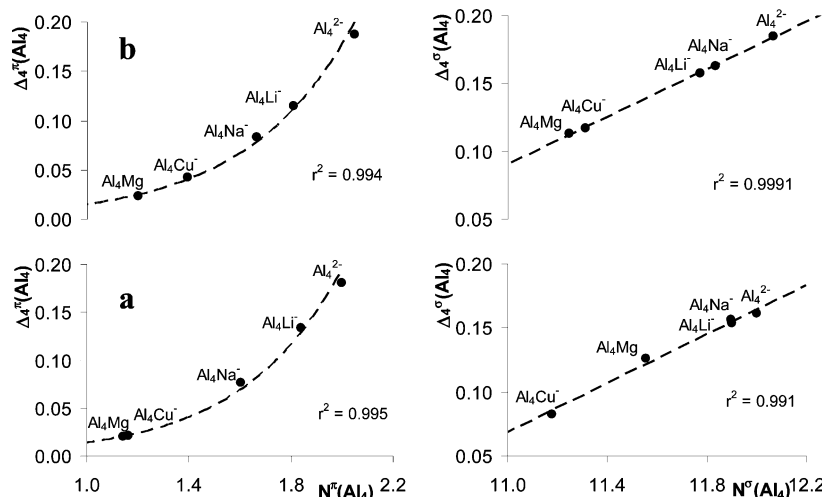
Figure 4. QTAIM (a) and Hirshfeld-I (b) σ and π 4-DIs vs the number of σ and π valence electrons of the Al_4 fragment in C_{4v} clusters.

al.[6] found that the π system of the Al_4^{2-} molecule, formed by two electrons in agreement with the Hückel's rule, is magnetically inactive. They also found a large magnetic activity of the σ system, attributing the major part of the aromaticity to the σ molecular orbitals. Magnetic ring current determinations pointed out that the $C_4H_4^{2+}$ system, also containing two π electrons, displays larger activity than the π system of Al_4^{2-}. On the contrary, the 4-DIs show that the π electron delocalization among the four Al atoms in Al_4^{2-} (0.1804 and 0.1875 for QTAIM and Hirshfeld-I, respectively) is quite similar to that of the four C atoms in $C_4H_4^{2+}$ (0.1804 and 0.1620 for QTAIM and Hirshfeld-I respectively). On the other hand, the σ electron delocalization is slightly smaller than the π one for Al_4^{2-} (0.1613 and 0.1850 for QTAIM and Hirshfeld-I, respectively). These results are in line with the π and σ components of the NICS index (−17.8 and −11.1) computed at the same level,[11] and also with the ELFπ and ELFσ bifurcation values calculated by Santos et al. (0.99 and 0.88, respectively), which reflect small larger contribution of the π electrons to the total aromaticity. It might thus appear that ring current maps and multicenter indices contradict each other. This is, however, not necessarily the case. First, Havenith et al.[7] have shown that the NICS data should be treated with care as the induced current from the π system is not a ring current and thus better not considered as indicating aromaticity. The magnetic properties can in fact all be related to the σ system. As the ring current is a response to an external perturbation, it also involves the virtual orbitals of appropriate symmetry. In this sense, a delocalized system is a necessary condition to have a ring current but not a sufficient one.[84] If there is no virtual orbital of correct symmetry within some energetically acceptable range from an occupied orbital in the unperturbed situation, no ring current will be found. So the fact that multicenter indices reveal both a σ and π delocalized system does not necessarily contradict ring current findings. In this

context, it should again be stressed that confronting conclusions from different studies of aromaticity should be done carefully, making sure that the concept of aromaticity reflects the same quantity. Multicenter indices reflect the delocalization aspect of a molecule whereas ring currents reflect a response property. In some molecules these are related, as for example in benzenoid rings,[54] but this is not generally true.

Looking at the local aromaticity of the Al_4 unit in the metal clusters in terms of 4-DIs, one finds that the σ and π local aromaticity is directly related to the σ and π electron populations. The splitting of the 4-DI for Al_4 into σ and π contributions can be done, in a good approximation, for systems where the Al_4 unit displays a planar geometry. Those systems are the C_{4v} clusters, which display one molecular orbital that shows approximate π symmetry with respect to the plane defined by the aluminum atoms (see Figure 3), and that can be identified as the π molecular orbital responsible for the π aromaticity in Al_4^{2-}. The calculation of the n-DIs for the C_{4v} clusters as summation of approximated s and p contributions leads to errors on the total 4-DIs lower than 2.6% using Hirshfeld-I partitioning, whereas they are lower than 5% using QTAIM partitioning. The only exception is the Al_4Cu cluster where the error is 18.3% for QTAIM, although it is only 1.5% for Hirshfeld-I.

In Figure 4 the values of σ and π 4-DIs for the Al_4 fragments are depicted versus the σ and π electron populations, calculated using the QTAIM and Hirshfeld-I partitionings. As one can see, the local aromaticity increases monotonously with the electron population. It is interesting to note that the σ aromaticity is linearly correlated with the number of σ electrons, whereas the π aromaticity shows an exponential decay. The σ aromaticity of the Al_4^{2-} is preserved in the alkaline metal clusters, whereas it decreases significantly in Al_4Cu^- and Al_4Mg. On the other hand, the π aromaticity of the Al_4 unit experiences a higher decrease than that of σ in all the clusters, as is expected from

TABLE 4: Relative Hirshfeld-I and QTAIM Energies of the Al$_4$ and M Fragments in kcal mol^{-1} (Details in Text)^a

| | $E(Al_4)$ | | $E(M)$ | | |
	QTAIM	Hirshfeld-I	QTAIM	Hirshfeld-I	E^{int}
Al$_4$Li$^-$	−139.8	−36.7	−68.5	−170.5	−211.1
Al$_4$Na$^-$	−150.2	−4.7	−44.4	−189.1	−198.2
Al$_4$Cu$^-$	481.7	209.7	−765.6	−494.2	−284.9
Al$_4$Be	−1.1	−29.1	−676.8	−649.0	−676.4
Al$_4$Mg	−138.6	−21.4	−410.8	−527.9	−550.2
Al$_4$Zn	492.1	106.5	−1141.7	−757.6	−649.6

^{a} The total interaction energies, E^{int}, between the Al$_4^{2-}$ and the cation M$^+$ or M^{2+} are listed in the last column.

the large overlapping between the π MO and the metal M (see Figure 3). The largest π aromaticity is shown again by the alkaline metal clusters.

It must be noted that the Al$_4$ fragments in the Al$_4$Be and Al$_4$-Zn clusters display the smallest 4-DIs according to the three atomic partitionings, indicating that they are the least aromatic Al$_4$ units. The strong covalent bonds shown by the Be and Zn atoms with one of the Al atoms breaks down the aromaticity of the Al$_4$ unit and give rise to a large geometry distortion of the cluster.

Energy Decomposition. Table 4 collects the QTAIM and Hirshfeld-I energies of the Al$_4$ fragment and the metal M. The energies are shown with regard to those of the isolated fragments. The isolated fragments are created by isolating the coordinates of the Al$_4$ fragments in the clusters and setting their charge and multiplicity to the ground state of the ^{1}Al$_4^{2-}$ dianion. The energies of those isolated fragments were calculated using the same basis set as in the clusters (Boys and Bernardi method).[85] In that way, the values of Table 4 represent the partitioning into molecular fragments of the total interaction energy (also included in the Table) between the ^{1}Al$_4^{2-}$ unit and the ground state of the metal M in its cationic form, M$^+$ or M^{2+}, depending on the total charge of the cluster. Thus, the results of Table 4 give information about the stability/instability of the Al$_4$ unit due to the new bonding situation. In addition, they provide a classification based on the energy of the different Al$_4$ fragments along the series. It must be noticed that we have also calculated the same relative energies using the ^{3}Al$_4^0$ as reference. Nevertheless, the energy difference between ^{3}Al$_4^0$ and ^{1}Al$_4^{2-}$ at the level of theory here employed is only 5.6 kcal mol^{-1}, so that the relative energies of the Al$_4$ fragments do not change significantly compared to the values shown in Table 4.

According to both QTAIM and Hirshfeld-I energies, the Al$_4$ fragment is stabilized by alkaline and alkaline earth metals, whereas it is clearly destabilized by transition metals. The destabilization of the Al$_4$ fragment in the transition metal clusters is compensated by the large stabilization of M, resulting in a total stabilization of the cluster (see Table 4). According to the QTAIM energies, the Al$_4$ unit can be classified into three groups: alkaline metal clusters and Al$_4$Mg, transition metal clusters, and the specific case of Al$_4$Be, which shows a small stabilization with regard to the reference. On the other hand, according to the Hirshfeld-I energies, the Al$_4$ unit can be classified approximately into two groups: alkaline metal and alkaline earth metal clusters, and transition metal clusters. The destabilization of the Al$_4$ fragment in the transition metal clusters cannot be attributed to the electron transfer because it is quite different in the Al$_4$Cu$^-$ and Al$_4$Zn. It must be noticed that the Al$_4$ displays very different energy in Al$_4$Be and Al$_4$Zn, even though these clusters display similar structure and charge polarization.
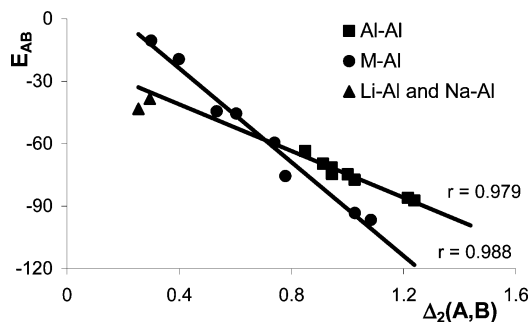
Figure 5. Hirshfeld-I 2-DIs, Δ_2(A,B), in au vs the 2-center energy terms, E_{AB}, in kcal mol^{-1}. The Al−Al and M−Al atomic pairs are represented respectively by boldface squares and boldface circles, whereas the Li−Al and Na−Al atomic pairs are represented by boldface triangles.

Although the total stability of the clusters also depends on the intra-atomic energy terms or one-center terms, one can intuitively state that the interatomic terms or two-center terms, resulting from the atomic energy partitioning, provide valuable information about the bond strength. Thus, information about the Hirshfeld-I interatomic and intra-atomic energies in the studied metal clusters is collected in Table 5. The strongest M−Al bonds are found in the C_s clusters and correspond to the shortest M−Al bond distances and largest 2-DIs, with E_{AB}(M−Al) values of −96.6 and −93.3 kcal mol^{-1} for Al$_4$Be and Al$_4$-Zn clusters, respectively. However, it is one of the C_{4v} clusters, Al$_4$Cu$^-$, which displays the largest total stability of the M−Al bonds, represented in Table 5 by the summation of all the E_{AB}-(M−Al) values. Looking at the summation of the E_{AB}(Al−Al) values, which are shown with respect to those of Al$_4^{2-}$, one can remark that the most destabilized Al−Al bonds are found in the C_s clusters, whereas the alkaline metal clusters display Al−Al interatomic energies close to those of Al$_4^{2-}$.

One can also extract some valuable information from the one-center terms. Thus, the "own energy" of the Al$_4$ fragments is represented by the summation of the intra-atomic and inter-atomic energy terms involving only Al atoms. These values are shown with regard to the energy of the Al$_4^{2-}$ in Table 5. One can see that all the relative values are positive, which indicates a destabilization of the "own energy" of the Al$_4$ unit. This is not a surprising result, because these values reflect the desta-bilization of the Al$_4$ unit due to the geometry distortion and electron charge donation, but these values do not reflect any stabilization due to the formation of new M−Al bonds. On the contrary, surprising results are found when adding the 2-center M−Al energy terms to the "own energy" of the Al$_4$. The resulting values are also included in Table 5 and shown with regard to the energy of the Al$_4^{2-}$. The stabilization given by the M−Al interatomic interactions is not enough to get a stable cluster when M is a transition metal (see the positive values for Al$_4$Cu and Al$_4$Zn); the opposite is found when M is an alkaline or alkaline earth metal. This implies that the intra-atomic energy of the metal, E_A(M) (not shown in Table 5), and its stabilization play a key role in the total stability of the cluster when the metal is a transition metal. The values from the last row in Table 5 reflect a clear relation between the relative destabilization of the Al$_4^{2-}$ and the size of the cation, being a bit larger for monocations. Mang et al.[86] investigated the relative stability of the square pyramidal conformations with regard to the planar ones for several Al$_4$M$^-$ all metal clusters. They found that the stability decreases with the size of the cation M$^+$, reversing the stability order for Au$^+$.

Finally, it would be desirable to find a good relation between the 2-DIs and the two-center energy terms, because both have

TABLE 5: Summation of Hirshfeld-I Two-Center, E_{AB}, and One-Center, E_A, Energy Terms Obtained for Several Fragments of the Metal Clusters Studied. All Values in kcal mol^{-1}.

	Al_4Li^-	Al_4Na^-	Al_4Cu^-	Al_4Be	Al_4Mg	Al_4Zn
$\Sigma E_A(Al)^a$	33.8	52.3	314.9	11.6	15.9	132.4
$\Sigma E_{AB}(Al-Al)^a$	11.8	15.5	48.9	79.3	55.8	72.7
$\Sigma E_{AB}(M-Al)$	−172.8	−153.6	−302.4	−235.3	−177.8	−194.8
$[\Sigma E_A(Al) + \Sigma E_{AB}(Al-Al)]^a$	45.6	67.8	363.9	90.9	71.7	205.2
$[\Sigma E_A(Al) + \Sigma E_{AB}(Al-Al) + \Sigma E_{AB}(M-Al)]^a$	−127.3	−85.8	61.5	−144.4	−106.1	10.4

^{a} Values relative to that of Al_4^{2-} (−969.1350 au and −379.7 kcal mol for respectively $\Sigma E_A(Al)$ and $\Sigma E_{AB}(Al-Al)$.

been used here to measure the bond strength between pairs of atoms. In Figure 5 the 2-DIs are depicted versus the two-center energy terms for all the bonds in all the clusters. The correlations obtained by separating the Al−Al bonds from the M−Al bonds are very good. Only the Li−Al and Na−Al bonds display deviations with regard to the rest of M−Al pairs. They show a larger stabilization than that predicted by the values of the 2-DIs. This is mainly due to the large ionic character of these bonds, which has been discussed at the beginning of this section. Because the 2-DI only provides a measure of the covalent character, they are expected to fail for highly ionic bonds. On the other hand, the slope of the representation for Al−Al bonds is smaller than that of M−Al bonds, meaning that the interatomic energies within the Al_4 fragments are less sensitive to changes in the 2-DIs, than the interatomic energies of fragments containing the metal M.

IV. Concluding Remarks

According to the calculated atomic charges and using an electronegativity scale, the QTAIM scheme provides a good description of the electron charge polarization in the all-metal clusters. According to the QTAIM results, alkaline metal clusters and to a lesser extent the Al_4Mg cluster exhibit large electron charge polarization from the metal, M, to the Al_4 unit and weak covalent M−Al bonds. On the contrary, the M−Al bonds exhibit strong covalent character in the less polarized clusters, Al_4Be Al_4Cu^- and Al_4Zn. The Hirshfeld-I results agree with the QTAIM ones, only some discrepancies are found for the atomic charges of transition metal clusters, especially for Al_4Cu^-. The Mulliken scheme does not provide a correct picture of the M−Al bonding in the alkaline metal clusters and Al_4Mg. However, it coincides with the QTAIM results for the transition metal clusters and Al_4Be. The three atomic partitioning schemes point out that the electron charge moves from the Al_4 unit to Be in Al_4Be, which disagrees with previously reported results obtained for the Al_4Be_4 system using ELF.

The QTAIM, Hirshfeld-I and Mulliken n-DIs of molecular fragments containing three, four, and five atoms are similar or even larger than those computed for π aromatic systems. This is a consequence of the electron sharing associated to the metallic character of these clusters. The multicenter delocalization indices prove to be a quantitative tool for characterizing the metallic bonding along the different molecular fragments. The Hirshfeld multicenter electron delocalization indices are successfully calculated for the first time.

The previously reported magnetic inactivity of the π system in the Al_4^{2-} cluster, based on means of magnetic ring currents, contrasts with its large π electron delocalization, which is the same as that of the $C_4H_4^{2+}$ molecule and slightly larger than that of the σ system. However, these results do not contradict each other, because a large electron delocalization is a necessary condition for the existence of ring currents but not a sufficient one. The magnitude of the π and σ aromaticity derived from the multicenter indices agrees with the previously reported ELF_π

and ELF_σ bifurcation values. The σ and π electron delocalization within the Al_4 unit in the series of metal clusters studied is shown to depend on the σ and π atomic electron populations and to decrease as the electron delocalization increases in fragments containing the metal M.

According to the QTAIM and Hirshfeld-I fragment energy, the Al_4^{2-} system is stabilized by the cations M^+/M^{2+} when M is a light alkaline or alkaline earth metal. On the contrary, it is destabilized by the transition metal cations. The stabilization of the complex is giving by the intra-atomic stabilization of the transition metal cation. A comparison of the interatomic energy terms with the 2-DIs reflects a linear correlation between both magnitudes for the M−Al and Al−Al bonds separately.

References and Notes

(1) Li, X.; Kuznetsov, A. E.; Zhang, H. F.; Boldyrev, A. I.; Wang, L. S. *Science* **2001**, *291*, 859.
(2) Kuznetsov, A. E.; Birch, K. A.; Boldyrev, A. I.; Li, X.; Zhai, H. J.; Wang, L. S. *Science* **2003**, *300*, 622.
(3) Boldyrev, A. I.; Wang, L-S. *Chem. Rev.* **2005**, *105*, 3716.
(4) Fowler, P. W.; Havenith, R. W. A.; Steiner, E. *Chem. Phys. Lett.* **2001**, *342*, 85.
(5) Fowler, P. W.; Havenith, R. W. A.; Steiner, E. *Chem. Phys. Lett.* **2002**, *359*, 530.
(6) Havenith, R. W. A.; Fowler, P. W.; Steiner, E.; Shetty, S.; Kanhere, D.; Pal, S. *Phys. Chem. Chem. Phys.* **2004**, *6*, 285.
(7) Havenith, R. W. A.; Fowler, P. W. *Phys. Chem. Chem. Phys.* **2006**, *8*, 3383.
(8) Juselius, J.; Straka, M.; Sundholm, D. *J. Phys. Chem. A* **2001**, *105*, 9939.
(9) Lin, Y.-C.; Juselius, J.; Sundholm, D.; Gauss, J. *J. Chem. Phys.* **2005**, *122*, 214308.
(10) Chen, Z.; Corminboeuf, C.; Bohmann, J.; Schleyer, P. v. R. *J. Am. Chem. Soc.* **2003**, *125*, 13930.
(11) Islas, R.; Heine, T.; Merino, G. *J. Chem. Theory Comput.* **2007**, *3*, 775.
(12) Havenith, R. W. A.; van Lenthe, J. H. *Chem. Phys. Lett.* **2004**, *385*, 198.
(13) Santos, J. C.; Tiznado, W.; Contreras, R.; Fuentealba, P. *J. Chem. Phys.* **2004**, *120*, 1670.
(14) Zhan, C.-G.; Zheng, F.; Dixon, D. A. *J. Am. Chem. Soc.* **2002**, *124*, 14795.
(15) Boldyrev, A. I.; Kuznetsov, A. E. *Inorg. Chem.* **2002**, *41*, 532.
(16) Chattaraj, P. K.; Roy, D. R.; Elango, M.; Subramanian, V. *J. Mol. Struct. (THEOCHEM)* **2006**, *759*, 109.
(17) Li, X.; Kuznetsov, A. E.; Zhang, H. F.; Boldyrev, A. I.; Wang, L. S. *Science* **2001**, *291*, 859.
(18) Power, P. P. Multiple Bonding Between Heavier Group 13 Elements. *Struct. Bonding* **2002**, *103*, 58.
(19) Li, X.; Zhang, H. F.; Wang, L. S.; Kuznetsov, A. E.; Cannon, N. A.; Boldyrev, A. I. *Angew. Chem., Int. Ed.* **2001**, *40*, 1867.
(20) Chi, X. X.; Li, X. H.; Chen, X. J.; Yuang, Z. S. *J. Mol. Struct. (THEOCHEM)* **2004**, *677*, 21.
(21) Zhao, C.; Balasubramanian, K. *J. Chem. Phys.* **2004**, *120*, 10501.
(22) Kuznetsov, A. E.; Boldyrev, A. I. *Struct. Chem.* **2002**, *13*, 141.

(23) Tanaka, H.; Neukermans, S.; Janssens, E.; Silverans, R. E.; Lievens, P. *J. Am. Chem. Soc.* **2003**, *125*, 2862.

(24) Alexandrova, A. N.; Boldyrev, A. I.; Zhai, H.-J.; Wang, L. S. *J. Phys. Chem. A* **2005**, *109*, 562.

(25) Wannere, C. S.; Corminboeuf, C.; Wang, Z.- X.; Wodrich, M. D.; King, R. B.; Schleyer, P. v. R. *J. Am. Chem. Soc.* **2005**, *127*, 5701.

(26) Tsipis, A. C.; Tsipis, C. A. *J. Am. Chem. Soc.* **2003**, *125*, 1136.

(27) Mercero, J. M.; Ugalde, J. M. *J. Am. Chem. Soc.* **2004**, *126*, 3380.

(28) Kong, Q.; Chen, M.; Dong, J.; Li, Z.; Fan, K.; Zhou, M. *J. Phys. Chem. A* **2002**, *106*, 11709.

(29) Kuznetsov, A. E.; Zhai, H. J.; Wang, L. S.; Boldyrev, A. I. *Inorg. Chem.* **2002**, *41*, 6062.

(30) Gausa, M.; Kaschner, R.; Lutz, H. O.; Seifert, G.; Meiwes-Broer, K.-H. *Chem. Phys. Lett.* **1994**, *230*, 99.

(31) Gausa, M.; Kaschner, R.; Seifert, G.; Faehmann, J. H.; Lutz, H. O.; Meiwes-Broer, K.-H. *J. Chem. Phys.* **1996**, *104*, 9719.

(32) Lein, M.; Frunzke, J.; Frenking, G. *Angew. Chem., Int. Ed.* **2003**, *42*, 1303.

(33) Zhai, H.-J.; Wang, L. S.; Kuznetsov, A. E.; Boldyrev, A. I. *J. Chem. Phys. A* **2002**, *106*, 5600.

(34) Shetty, S.; Dilip, G. K.; Pal, S. *J. Phys. Chem. A* **2004**, *108*, 628.

(35) Tsipis, C. A. *Coord. Chem. Rev.* **2005**, *249*, 2740.

(36) Nigam, S.; Majumder, C.; Kulshreshtha, S. K. *J. Mol. Struct. (THEOCHEM)*, **2005**, *755*, 187.

(37) Shetty, S.; Pal, S.; Kanhere, D. G. *J. Chem. Phys.* **2003**, *118*, 7288.

(38) Fradera, X.; Austen, M. A.; Bader, R. F. W. *J. Phys. Chem. A* **1999**, *103*, 304.

(39) Giambiagi, M.; De Giambiagi, M. S.; Grempel, D. R.; Heymann, C. D. *J. Chim. Phys.* **1975**, *72*, 15.

(40) Mayer, I. *Chem. Phys. Lett.* **1983**, *97*, 270.

(41) Mundim, K. C.; Giambiagi, M.; De Giambiagi, M. S. *J. Phys. Chem.* **1994**, *98*, 6118.

(42) Ponec, R.; Mayer, I. *J. Phys. Chem. A* **1997**, *101*, 1738.

(43) Bochicchio, R. C.; Ponec, R.; Lain, L.; Torre, A. *J. Phys. Chem. A* **1998**, *102*, 7176.

(44) Ponec, R.; Torre, A.; Lain, L.; Bochicchio, R. C. *Int. J. Quantum Chem.* **2000**, *77*, 710.

(45) Torre, A.; Lain, L.; Bochicchio, R. C.; Ponec, R. *J. Comput. Chem.* **1999**, *20*, 1085.

(46) Bollini, C. G.; Giambiagi, M.; De Giambiagi, M. S.; De Figueiredo, A. P. *J. Mater. Chem.* **2000**, *28*, 71.

(47) Bollini, C. G.; Giambiagi, M.; De Giambiagi, M. S.; De Figueiredo, A. P. *Struct. Chem.* **2001**, *12*, 113−120.

(48) Giambiagi, M.; De Giambiagi, M. S.; Dos Santos Silva, C. D.; De Figueiredo, A. P. *Phys. Chem. Chem. Phys.* **2000**, *2*, 3381−3392.

(49) Bultinck, P.; Rafat, M.; Ponec, R.; Van Gheluwe, B.; Carbo-Dorca, R.; Popelier, P. L. A. *J. Phys. Chem. A* **2006**, *110*, 7642.

(50) Bultinck, P.; Mandado, M; Mosquera, R. A. *J. Math. Chem.* Published online (DOI: 10.1007/s10910-006-9184-8).

(51) Bultinck, P.; Ponec, R.; Van Damme, S. *J. Phys. Org. Chem.* **2005**, *18*, 706.

(52) Ponec, R.; Bultinck, P.; Gallegos, A. *J. Phys. Chem. A* **2005**, *109*, 6606.

(53) Bultinck, P.; Ponec, R.; Carbó-Dorca, R. *J. Comput. Chem.* **2007**, *28*, 152.

(54) Bultinck, P.; Fias, S.; Ponec, R. *Chem. Eur. J.* **2006**, *12*, 8813.

(55) Caramori, G. F.; de Oliveira, K. T.; Galembeck, S. E.; Bultinck, P.; Constantino, M. G. *J. Org. Chem.* **2007**, *72*, 76.

(56) Mandado, M.; González-Moa, M. J.; Mosquera, R. A. *J. Comput. Chem.* **2007**, *28*, 127.

(57) Mandado, M.; González-Moa, M. J.; Mosquera, R. A. *J. Comput. Chem.* **2007**, *28*, 1625.

(58) Mandado, M.; Otero, N.; Mosquera, R. A. *Tetrahedron* **2006**, *62*, 12204.

(59) Mandado, M.; González-Moa, M. J.; Mosquera, R. A. *Chem. Phys. Chem.* **2007**, *8*, 696.

(60) Mandado, M.; Bultinck, P.; González-Moa, M. J.; Mosquera, R. A. *Chem. Phys. Lett.* **2006**, *433*, 5.

(61) Mulliken, R. S. *J. Chem. Phys.* **1955**, *23*, 1833.

(62) Bader, R. F. W. *Atoms in Molecules - A Quantum Theory, International Series of Monographs on Chemistry*; Oxford University Press: Oxford 1990; No. 22.

(63) Hirshfeld, F. L. *Theor. Chim. Acta* **1977**, *44*, 129.

(64) Mundim, K. C.; Giambiagi, M.; de Giambiagi, M. S. *J. Phys. Chem.* **1994**, *98*, 6118.

(65) Ponec, R.; Uhlik, F. *Croat. Chem. Acta* **1996**, *69*, 941.

(66) Poater, J.; Duran, M.; Solà, M.; Silvi, B. *Chem. Rev.* **2005**, *105*, 3911.

(67) Mandado, M.; Van, Alsenoy, C.; Geerlings, P.; De Proft, F.; Mosquera, R. A. *Chem. Phys. Chem.* **2006**, *7*, 1294.

(68) Cioslowski, J.; Liu, G. *Chem. Phys. Lett.* **1997**, *277*, 299.

(69) Pendás, A. M.; Blanco, M. A.; Francisco, E. *J. Chem. Phys.* **2004**, *120*, 4581.

(70) Pendás, A. M.; Francisco, E.; Blanco, M. A. *J. Comput. Chem.* **2005**, *26*, 344.

(71) Francisco, E.; Pendás, A. M.; Blanco, M. A. *J. Chem. Theory Comput.* **2006**, *2*, 90.

(72) Mayer, I.; Hamza, A. *Theor. Chem. Acc.* **2001**, *105*, 360.

(73) Salvador, P.; Duran, M.; Mayer, I. *J. Chem. Phys.* **2001**, *115*, 1153.

(74) Salvador, P.; Mayer, I. *J. Chem. Phys.* **2004**, *120*, 5046.

(75) Frisch, M. J.; Trucks, G. W.; Schlegel, H. B.; Scuseria, G. E.; Robb, M. A.; Cheeseman, J. R.; Montgomery, J. A., Jr.; Vreven, T.; Kudin, K. N.; Burant, J. C.; Millam, J. M.; Iyengar, S. S.; Tomasi, J.; Barone, V.; Mennucci, B.; Cossi, M.; Scalmani, G.; Rega, N.; Petersson, G. A.; Nakatsuji, H.; Hada, M.; Ehara, M.; Toyota, K.; Fukuda, R.; Hasegawa, J.; Ishida, M.; Nakajima, T.; Honda, Y.; Kitao, O.; Nakai, H.; Klene, M.; Li, X.; Knox, J. E.; Hratchian, H. P.; Cross, J. B.; Bakken, V.; Adamo, C.; Jaramillo, J.; Gomperts, R.; Stratmann, R. E.; Yazyev, O.; Austin, A. J.; Cammi, R.; Pomelli, C.; Ochterski, J. W.; Ayala, P. Y.; Morokuma, K.; Voth, G. A.; Salvador, P.; Dannenberg, J. J.; Zakrzewski, V. G.; Dapprich, S.; Daniels, A. D.; Strain, M. C.; Farkas, O.; Malick, D. K.; Rabuck, A. D.; Raghavachari, K.; Foresman, J. B.; Ortiz, J. V.; Cui, Q.; Baboul, A. G.; Clifford, S.; Cioslowski, J.; Stefanov, B. B.; Liu, G.; Liashenko, A.; Piskorz, P.; Komaromi, I.; Martin, R. L.; Fox, D. J.; Keith, T.; Al-Laham, M. A.; Peng, C. Y.; Nanayakkara, A.; Challacombe, M.; Gill, P. M. W.; Johnson, B.; Chen, W.; Wong, M. W.; Gonzalez, C.; Pople, J. A. *Gaussian 03*, revision C.02; Gaussian, Inc.: Wallingford, CT, 2004.

(76) *AIMPAC: A suite of programs for the Theory of Atoms in Molecules*; Bader, R. F. W., et al., Eds.; McMaster University, Hamilton, Ont., Canada L8S 4M1. Contact: bader@mcmail.cis.mcmaster.ca.

(77) Van, Alsenoy, C.; Peeters, A. *THEOCHEM* **1993**, *286*, 19.

(78) Van, Alsenoy, C. *J. Comput. Chem.* **1988**, *9*, 620.

(79) Biegler-König, F. W.; Schönbohm, J.; Bayles, D. *J. Comput. Chem.* **2001**, *22*, 545.

(80) Bultinck, P.; Van Alsenoy, C.; Ayers, P. W.; Carbó-Dorca, R. *J. Chem. Phys.* **2007**, *126*, 144111.

(81) Bultinck, P.; Ayers, P. W.; Fias, S.; Tiels, K.; Van, Alsenoy, C. *Chem. Phys. Lett.* **2007**, *444*, 205.

(82) Jensen, F. *Introduction to Computational Chemistry*, 2th ed.; John Wiley & Sons: New York, 1999.

(83) Ponec, R.; Cooper, D. L. *J. Mol. Struct. (THEOCHEM)* **2005**, *727*, 133.

(84) Bultinck, P. A. *Faraday Discuss.* **2007**, *135*, 347.

(85) Boys, S. F.; Bernardi, F. *Mol. Phys.* **1978**, *19*, 553.

(86) Mang, C.; Liu, C.; Zhou, J.; Li, Z.; Wu, K. *Chem. Phys. Lett.* **2007**, *438*, 20.